

A Model of Visual Adaptation for Realistic Image Synthesis

James A. Ferwerda Sumanta N. Pattanaik Peter Shirley Donald P. Greenberg

Program of Computer Graphics, Cornell University*

Abstract

In this paper we develop a computational model of visual adaptation for realistic image synthesis based on psychophysical experiments. The model captures the changes in threshold visibility, color appearance, visual acuity, and sensitivity over time that are caused by the visual system's adaptation mechanisms. We use the model to display the results of global illumination simulations illuminated at intensities ranging from daylight down to starlight. The resulting images better capture the visual characteristics of scenes viewed over a wide range of illumination levels. Because the model is based on psychophysical data it can be used to predict the visibility and appearance of scene features. This allows the model to be used as the basis of perceptually-based error metrics for limiting the precision of global illumination computations.

CR Categories and Subject Descriptors: I.3.0 [Computer Graphics]: General; I.3.6 [Computer Graphics]: Methodology and Techniques.

Additional Key Words and Phrases: realistic image synthesis, vision, visual perception, adaptation.

1 Introduction

The goal of realistic image synthesis is to produce images that capture the visual appearance of modeled scenes. Physically-based rendering methods make it possible to accurately simulate the distribution of light energy in scenes, but physical accuracy in rendering does not guarantee that the displayed images will have a realistic visual appearance. There are at least two reasons for this. First, the range of light energy in the scene may be vastly different from the range that can be produced by the display device. Second, the visual states of the scene observer and the display observer may be very different.

To produce realistic images we need to model not only the physical behavior of light propagation, but also the parameters of perceptual response. This is particularly true of the visual system's adaptation to the range of light we encounter in the natural environment since visual function changes dramatically over the range of environmental illumination.

*580 Frank H. T. Rhodes Hall, Ithaca, NY 14853, USA.
<http://www.graphics.cornell.edu>.

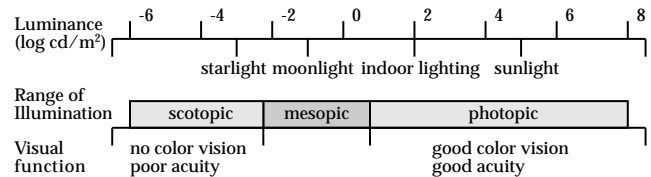


Figure 1: The range of luminances in the natural environment and associated visual parameters. After Hood (1986).

Very little work has been done in computer graphics on adaptation. Earlier work has focused primarily on overcoming the limits of conventional CRT displays and determining how to best display simulated environments within the limited dynamic range available. Tumblin and Rushmeier (1993) introduced the concept of tone reproduction to the computer graphics community and developed a tone reproduction operator that preserves the apparent brightness of scene features. Ward (1994) has taken a somewhat different approach and has developed a tone reproduction operator that preserves apparent contrast and visibility. Spencer (1995) has developed a psychophysical model of glare and has implemented a glare filter that increases the apparent dynamic range of images.

The model of adaptation presented herein deals with many more visual parameters than dynamic range. We develop a model that includes the effects of adaptation on *threshold visibility*, *color appearance*, *visual acuity*, and *changes in visual sensitivity over time*. The algorithm we derive from our model is based on the psychophysics of adaptation measured in experimental studies. Therefore, it can be used predictively for illumination engineering work, and can be used to develop perceptually-based approaches to rendering and display.

1.1 Background

The range of light energy we experience in the course of a day is vast. The light of the noonday sun can be as much as 10 million times more intense than moonlight. Figure 1 shows the range of luminances we encounter in the natural environment and summarizes some visual parameters associated with this luminance range. Our visual system copes with this huge range of luminances by adapting to the prevailing conditions of illumination. Through adaptation the visual system functions over a luminance range of nearly 14 log units.

Adaptation is achieved through the coordinated action of mechanical, photochemical, and neural processes in the visual system. The pupil, the rod and cone systems, bleaching and regeneration of receptor photopigments, and changes in neural processing all play a role in visual adaptation.

Although adaptation provides visual function over a wide range of ambient intensities, this does not mean that we see equally well at all intensity levels. For example, under dim

illumination our eyes are very sensitive, and we are able to detect small differences in luminance, however our acuity for pattern details and our ability to distinguish colors are both poor. This is why it is difficult to read a newspaper at twilight or to correctly choose a pair of colored socks while dressing at dawn. Conversely, in daylight we have sharp color vision, but absolute sensitivity is low and luminance differences must be great if we are to detect them. This is why it is impossible to see the stars against the sunlit sky.

Further, adaptation does not happen instantaneously. Nearly everyone has experienced the temporary blindness that occurs when you enter a dark theatre for a matinee. It can sometimes take a few minutes before you can see well enough to find an empty seat. Similarly, once you have dark adapted in the theatre and then go out into the daylight after the show, the brightness is at first dazzling and you need to squint or shield your eyes, but within about a minute, you can see normally again.

To produce realistic synthetic images that capture the appearance of actual scenes, we need to take adaptation-related changes in vision into account. In this paper we develop a computational model of visual adaptation and apply it to the problem of rendering scenes illuminated at vastly different levels. The model predicts the visibility of object features and colors at particular illumination levels, and simulates the changes in visibility and appearance that occur over the time-course of light and dark adaptation.

2 Physiological foundations of adaptation

Through adaptation the visual system functions over a luminance range of nearly 14 log units, despite the fact that the individual neural units that make up the system have a response range of only about 1.5 log units (Spillman 1990). Through four distinct adaptation mechanisms, the visual system moderates the effects of changing levels of illumination on visual response to provide sensitivity over a wide range of ambient light levels.

2.1 The pupil

The most obvious mechanism available to regulate the amount of light stimulating the visual system is the pupil. Over a 10 log unit range of luminance, the pupil changes in diameter from approximately 7 mm down to about 2 mm (Pugh 1988). This range of variation produces a little more than a log unit change in retinal illuminance so pupillary action alone is not sufficient to completely account for visual adaptation (Spillman 1990). In fact, rather than playing a significant role in adaptation it is thought that variation in pupil size serves to mitigate the visual consequences of aberrations in the eye's optical system. At high levels where there is plenty of light to see by, the pupil stops down to limit the effects of the aberrations. At low levels where catching enough light to allow detection is more essential than optimizing the resolution of the retinal image, the pupil opens to allow more light into the eye.

2.2 The rod and cone systems

There are somewhere between 75 and 150 million rod and 6 to 7 million cone photoreceptors in each retina (Riggs 1971). The rods are extremely sensitive to light and provide achromatic vision at *scotopic* levels of illumination ranging from 10^{-6} to 10 cd/m^2 . The cones are less sensitive than the rods, but provide color vision at *photopic* levels of illumination in

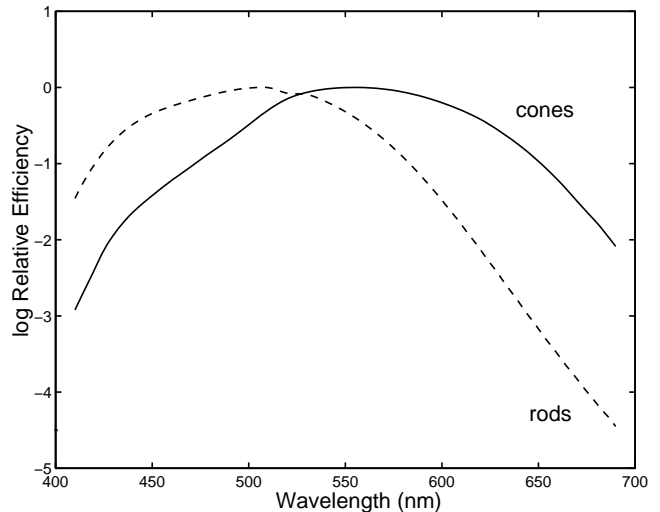


Figure 2: Scotopic V'_λ and photopic V_λ luminous efficiency functions. After Wyszecki (1982).

the range of 0.01 to 10^8 cd/m^2 . At light levels from 0.01 to 10 cd/m^2 both the rod and cone systems are active. This is known as the *mesopic* range. Relatively little is known about vision in the mesopic range but this is increasingly a topic of interest because computer-based office environments with CRT displays and subdued lighting exercise the visual system's mesopic range.

The rod and cone systems are sensitive to light with wavelengths from about 400nm to 700nm. The rods have their peak sensitivity at approximately 505nm. Spectral sensitivity of the composite cone system peaks at approximately 555 nm. The rod and cone systems are not equally sensitive to light at all wavelengths. *Luminous efficiency functions* show how effective light of a particular wavelength is as a visual stimulus. Differences between the rod and cone systems lead to separate photopic and scotopic luminous efficiency functions that apply to typical daytime and nighttime illumination levels. Figure 2 shows the normalized scotopic and photopic luminous efficiency functions developed by the CIE (Wyszecki 1982).

2.3 Bleaching and regeneration of photopigments

At high light intensities, the action of light depletes the photosensitive pigments in the rods and cones at a faster rate than chemical processes can restore them. This makes the receptors less sensitive to light. This process is known as *pigment bleaching*. Early theories of adaptation were based on the idea that light adaptation was produced by pigment bleaching and dark adaptation was produced by pigment restoration (Hecht 1934). However pigment bleaching cannot completely account for adaptation for two reasons: first, a substantial amount of adaptation takes place in both the rod and cone systems at ambient levels where little bleaching occurs (Granit 1939); and second, the time courses of the early phases of dark and light adaptation are too rapid to be explained by photochemical processes alone (Crawford 1947).

2.4 Neural processes

The neural response produced by a photoreceptor cell depends on chemical reactions produced by the action of light on the cell's photopigments. The cell's response to light is limited by the maximum rate and intensity of these chemical reactions. If the reactions are occurring near their maximum levels, and the amount of light striking the photopigments is increased, the cell may not be able to fully signal the increase. This situation is known as *saturation*. The result of saturation is *response compression*: above a certain level incremental increases in light intensity will produce smaller and smaller changes in the cell's response rate.

The rod and cone photoreceptors connect through a network of neurons in the retina to ganglion cells whose axons form the optic nerve. Adaptive processes sited in this neural network adjust the base activity and gain of the early visual system to mitigate the effects of response compression in the photoreceptors. A *multiplicative process* adjusts the gain of the system by effectively scaling the input by a constant related to the background luminance. This process acts very rapidly and accounts for changes in sensitivity over the first few seconds of adaptation. A slower acting *subtractive process* reduces the base level of activity in the system caused by a constant background. This process accounts for the slow improvement in sensitivity measured over minutes of adaptation (Adelson 1982).

3 A psychophysical model of adaptation

The physiological mechanisms described above provide the basis for visual adaptation. The action of these mechanisms is reflected in the changes in visibility, color appearance, visual acuity, and sensitivity over time that can be observed in everyday experience and measured in psychophysical experiments. In this section we will review a series of experiments that measure the changes in visual function that accompany adaptation. The results of these experiments will serve as the basis of our computational model of adaptation.

3.1 Threshold studies

Visual sensitivity is often measured psychophysically in a *detection threshold* experiment. In the typical experimental paradigm, an observer is seated in front of a blank screen that fills their field of view. To determine the absolute threshold the screen is made dark. To determine the contrast threshold a large region of the screen is illuminated to a particular background luminance level. Before testing begins, the observer fixates the center of the screen until they are completely adapted to the background level. On each trial a disk of light is flashed near the center of fixation for a few hundred milliseconds. The observer reports whether they see the disk or not. If the disk is not seen its intensity is increased on the next trial. If it is seen, its intensity is decreased. In this way, the detection threshold for the target disk against the background is measured.

There are many stimulus parameters that affect detection thresholds. Background and target size, color, duration, and position all affect threshold magnitude. To allow comparison of the different experiments in this section we have summarized the experimental parameters in insets on each graph. We have also converted from the diverse range of luminance and illuminance units used in the literature to a standard scale of $\log \text{cd/m}^2$ taking into account the changes in retinal

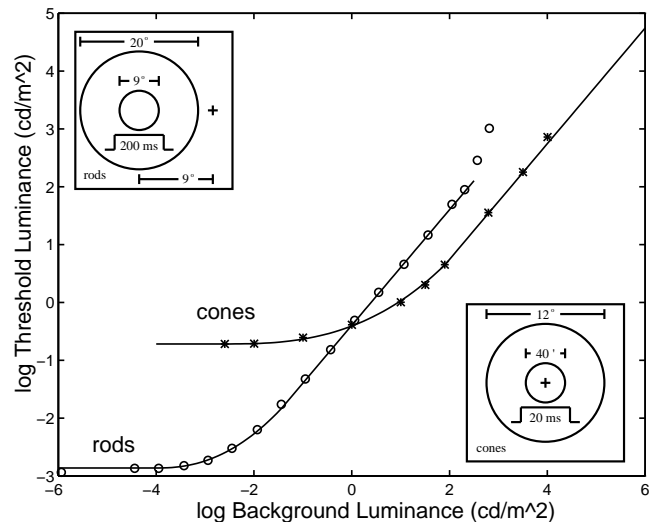


Figure 3: A psychophysical model of detection thresholds over the full range of vision.

illuminance due to changes in pupil size and differences in the luminous efficiency of the rod and cone systems.

3.2 Changes in threshold sensitivity

As the luminance of the background in a detection threshold experiment is increased from zero, the luminance difference between target and background required for detection increases in direct proportion to the background luminance. Plotting the detection threshold against the corresponding background luminance gives a *threshold-versus-intensity (t.v.i.)* function. Figure 3 shows the psychophysically measured t.v.i. functions for the rod and cone systems.

At luminance levels below about $-4 \log \text{cd/m}^2$, the rod curve flattens to a horizontal asymptote. This indicates that the luminance of the background has little effect on the threshold which approaches the limit for detecting a stimulus in the dark. At levels above $2 \log \text{cd/m}^2$ the curve approaches a vertical asymptote. This indicates that the rod system is being overloaded by the background luminance with the result that no amount of luminance difference between the background and target will allow detection.

Over a wide middle range covering 3.5 log units of background luminance the function is linear, this relationship can be described by the function $\Delta L = kL$. This relationship is known as *Weber's law* (Riggs 1971). Weber's law behavior is indicative of a system that has constant contrast sensitivity, since the proportional increase in threshold with increasing background luminance corresponds to a luminance pattern with constant contrast.

The other curve in Figure 3 shows the t.v.i. function for the cone system. In many ways the rod and cones show similar patterns of response. At levels below $-2.6 \log \text{cd/m}^2$, the t.v.i function is essentially flat indicating that the background has no effect on the response threshold. In this region the cones are operating at their absolute levels of sensitivity. At background levels above $2 \log \text{cd/m}^2$ the function is linear, indicating Weber's law behavior and constant contrast sensitivity. One important difference between the rod and cone functions is that the cone system never saturates in the upper reaches of the luminance range. Instead, pigment bleaching gradually lowers sensitivity all the way up

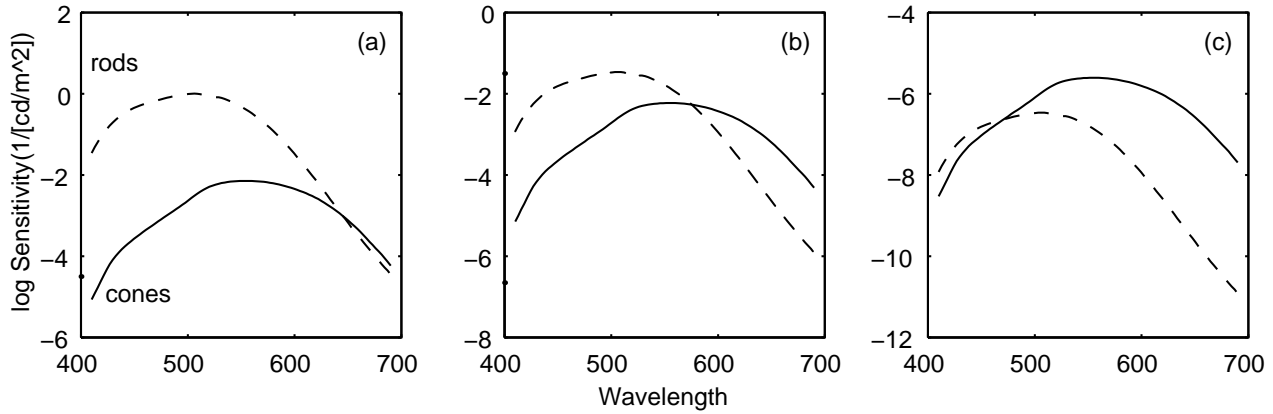


Figure 4: Changes in the spectral sensitivity of the visual system at (a) scotopic, (b) mesopic, and (c) photopic illumination levels. After Hood (1986).

to damaging intensity levels.

We have placed the rod and cone t.v.i. functions on the same graph to show the relative sensitivities of the systems and to show how threshold sensitivity varies over a wide range of scotopic and photopic background luminances. At background luminances from about -6 to 0 log cd/m^2 the rod system is more sensitive than the cone system. In this range the rods account for the magnitude of the detection threshold. As the background luminance is increased, the rod system loses sensitivity and the detection threshold rises. At a background level around 0 log cd/m^2 the rod and cone t.v.i. functions cross. Above this level the cone system is more sensitive than the rod system and it accounts for the detection threshold. Over a wide range of background luminances the visual system's threshold sensitivity can be described by the envelope of the rod and cone t.v.i. curves.

3.3 Changes in color appearance

The spectral sensitivities of the rod and cone systems are described by the scotopic and photopic luminous efficiency functions. When presented graphically, the functions are typically normalized which masks the fact that the rod and cone systems differ greatly in sensitivity and operate over different luminance ranges.

Figure 4 (a) shows the visual system's spectral sensitivity at scotopic levels. At these levels detection is dominated by the rod system. Absolute sensitivity is quite high, but since the rod system is achromatic, color will not be apparent.

Figure 4 (b) shows spectral sensitivity at mesopic levels. Here the rod and cone systems are nearly equal in absolute sensitivity. Detection at a particular wavelength will be served by the more sensitive system. The graph shows that the rods will detect wavelengths below about 575 nm and the cones will detect wavelengths above this point.

Figure 4 (c) shows the visual system's spectral sensitivity at photopic levels. At these levels detection is dominated by the cone system. Absolute sensitivity has dropped considerably, but due to the trichromatic nature of the cone system, colors will now be seen.

Figure 5 shows the luminous efficiency functions as surfaces positioned with respect to the rod and cone system threshold sensitivities at different luminance levels. This 3d graph shows how the visual system's spectral sensitivity changes with changing luminance levels and which system is dominant at a particular level. The subfigures show cross

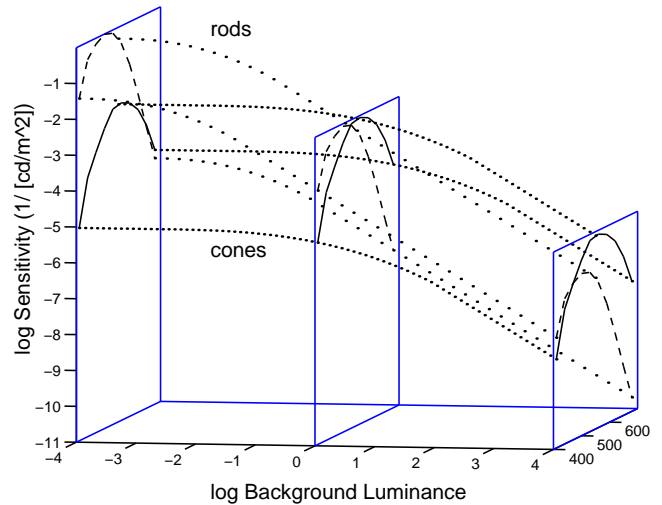


Figure 5: A model of threshold sensitivity as a function of wavelength and background luminance for the rod and cone systems.

sections of these spectral sensitivity vs. luminance surfaces.

This model of the changes in spectral sensitivity with changing luminance levels can account for a number of different color appearance phenomena observed over the scotopic to photopic range. First, at low luminance levels vision will be achromatic since detection at all wavelengths is served by the rod system. As the luminance level is raised into the mesopic range, the cone system will become active and colors will begin to be seen beginning with the long wavelength reds and progressing toward the middle wavelength greens. Only at relatively high luminances will short wavelength blue targets begin to appear colored.

3.4 Changes in visual acuity

Acuity is a measure of the visual system's ability to resolve spatial detail. Acuity is often measured clinically with the Snellen chart. A portion of the Snellen chart is shown in Figure 6. The letters of the chart are constructed such that the strokes of each character subtend precise visual angles when viewed from a distance of 20 feet. The bottom line

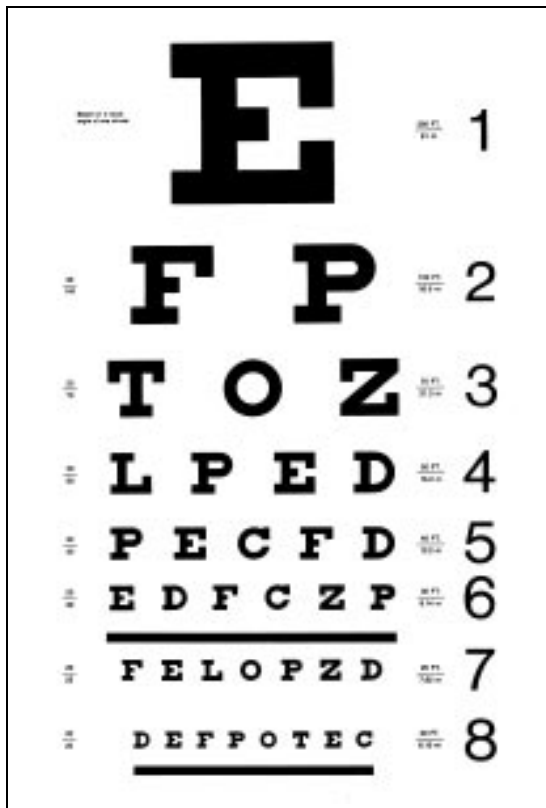


Figure 6: The Snellen acuity chart.

of the chart is taken as the standard of normal acuity. At 20 feet each character stroke in the bottom line (8) subtends one minute of visual angle. A viewer who can correctly identify the characters on this line is said to have 20/20 vision. The upper lines in the chart have progressively wider stroke widths. These lines are used to assess subnormal acuity. For example each stroke in the characters on line 5 is twice as big as those on line 8. A person with normal acuity can identify the characters in this line from a distance of 40 feet. If you can just identify this line at the standard 20 foot viewing distance then you have 20/40 vision. The large E on line 1 of the chart is equivalent to a visual acuity of 20/200.

Acuity is lower at scotopic levels of illumination than at photopic levels. The curve in Figure 7 shows how visual acuity changes with background luminance. The data cover the range from daylight down to starlight. The experiment measured acuity by testing the detectability of square wave gratings of different spatial frequencies. The graph shows that the highest frequency grating that can be resolved drops from a high of about 50 cycles/degree at $3 \log \text{cd/m}^2$ down to about 2 cycles/degree at $-3.3 \log \text{cd/m}^2$. This is equivalent to a change from almost 20/10 vision at daylight levels down to nearly 20/300 under starlight. This curve can be used to predict the visibility of scene details at different levels of illumination. At low levels of illumination it should be difficult to resolve detailed patterns, like the smaller lines on the Snellen chart or fine textures.

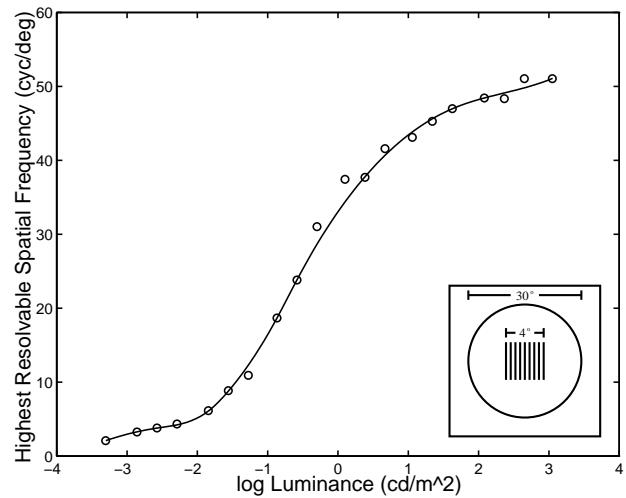


Figure 7: Changes in grating acuity as a function of background luminance. After Shaler (1937).

3.5 The time-course of adaptation

3.5.1 Light adaptation

Adaptation does not happen instantaneously. If you are seated in a dark room and the lights are suddenly switched on it takes several seconds before you adjust to seeing at the new level of illumination. This process is known as *light adaptation*. Figure 8 shows the results of an experiment on the time course of light adaptation in the rod system (Adelson 1982). Prior to the experiment the observer was dark adapted. At the beginning of the experiment a large background field of $0.5 \log \text{cd/m}^2$ was switched on and from that moment forward the threshold was measured repeatedly. In the instant after the background field was switched on the detection threshold jumped from its dark adapted level to about $0.1 \log \text{cd/m}^2$, but after 2 seconds the threshold has dropped back to about $-1.7 \log \text{cd/m}^2$. The graph shows that light adaptation in the scotopic range of the rod system is extremely rapid. More than 80% of sensitivity recovery occurs within the first 2 seconds, and nearly 75% happens within the first 200 ms.

Figure 9 shows the results of a similar experiment on the time-course of light adaptation in the cone system (Baker 1949). As with the rod system, thresholds are highest immediately after the onset of the background field. At a $3.75 \log \text{cd/m}^2$ background level, the instantaneous threshold is about $3.5 \log \text{cd/m}^2$. The threshold decreases over time and reaches a minimum after about 3 minutes of exposure. The threshold drops more than 0.5 log units during this period. After 3 minutes the threshold rises again slightly (due to interactions between neural and photochemical processes in adaptation) and reaches its fully adapted level at about 10 minutes. This experiment also shows that the time course of light adaptation in the cone system is slower than the rod system.

Visually, light adaptation provides a distinctive experience. When we go quickly from low to high levels of illumination, at first everything is painfully glaring and we squint or close one eye to reduce the discomfort. However over time the overall brightness of the visual field diminishes to more comfortable levels and normal vision is restored.

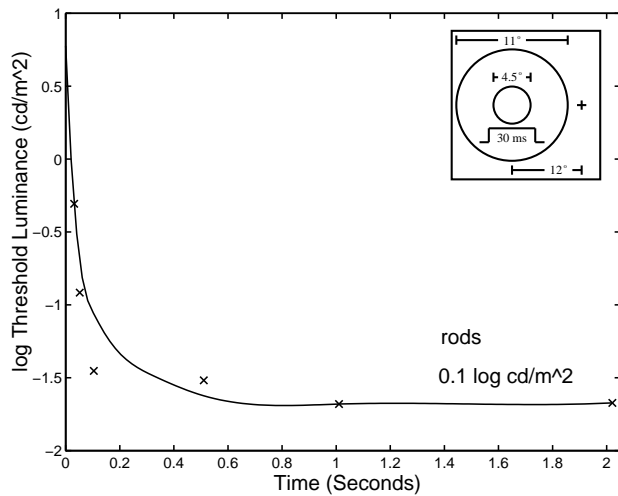


Figure 8: The time course of light adaptation in the rod system. After Adelson (1982).

3.5.2 Dark adaptation

Figure 10 shows the time-course of *dark adaptation* as measured by Hecht (1934). In this experiment, the observer was first adapted to a high background luminance and then plunged into darkness. Detection thresholds were measured continuously over more than 30 minutes. The graph shows the detection threshold as a function of time in the dark. The kinked threshold curve is actually the envelope of the curves for the separately tested rod and cone systems. In the first 5 minutes after the adapting field is switched off, the threshold drops rapidly, but then it levels off at a relatively high level because the cone system has reached its greatest sensitivity, but the rod system has still not recovered significantly. After about 7 minutes rod system sensitivity surpasses that of the cone system and the threshold begins to drop again. This point is known as the *Purkinje break* (Riggs 1971) and indicates the transition from detection by the cone system to detection by the rods. Changes in the threshold can be measured out to about 35 minutes, at which point the visual system has reached its absolute levels of sensitivity, and the threshold has dropped nearly 4 log units.

Visually, dark adaptation is experienced as the temporary blindness that occurs when we go rapidly from photopic to scotopic levels of illumination. The relatively slow time-course of dark adaptation means that vision can be impaired for several minutes when we move quickly from high illumination levels to low ones.

3.6 Summary

The cumulative achievement of adaptation is that the visual system is sensitive over a vast range of ambient light levels despite severe limits on the dynamic ranges of the individual neural units that make up the system. However this does not mean that we see equally well at all levels of illumination. The experiments show that threshold visibility, color appearance, and visual acuity are different at different illumination levels, and that these visual parameters change over the time-course of light and dark adaptation.

We will now develop a computational model of the changes in threshold visibility, color appearance, visual acuity, and sensitivity over time that are given by the experiments de-

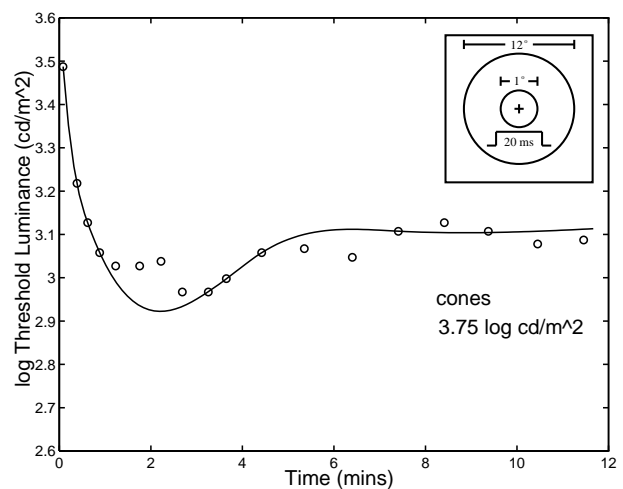


Figure 9: The time course of light adaptation in the cone system. After Baker (1949).

scribed above. This computational model will allow us to produce synthetic images that better capture the appearance of scenes illuminated at different levels. Because the computational model is based on psychophysical data, it will allow us to predict the visibility, color appearance, and clarity of scene features at a given level of illumination and to describe the changes in these visual parameters over the time-courses of light and dark adaptation.

4 Implementation

We implement our model in a program that maps image files with photopic luminance (CIE Y), scotopic luminance, and CIE XZ channels to displayable images in a fixed RGB color space. Since this is fundamentally a tone reproduction problem, our algorithm draws on the state-of-the-art in this area.

Tumblin and Rushmeier (1993) introduced the concept of *tone reproduction* to the computer graphics community. Tone reproduction addresses the goal of making an image that is a faithful visual representation of the photometric properties of a scene. Tone reproduction operators describe the mapping from scene to display in terms of physical processes in the display system and psychophysical processes in hypothetical scene and display viewers that affect the fidelity of the displayed image to the scene.

Tumblin and Rushmeier developed a tone reproduction operator that preserves *brightness* relationships. Their operator uses a psychophysical model of brightness perception developed by Stevens and Stevens (1960) to produce a mapping from scene luminances to display luminances such that the perceived brightness of a region on the display will match the perceived brightness of a region in the scene.

A somewhat different approach to tone reproduction has been developed by Ward (1994). Ward's operator differs from Tumblin and Rushmeier's in that it preserves perceived *contrast* rather than perceived brightness. Ward's operator is based on threshold contrast sensitivity data collected by Blackwell (CIE 1981). The operator maps *just noticeable contrast differences* (JND's) in the scene to just noticeable differences in the image.

From a psychophysical point of view, Tumblin and

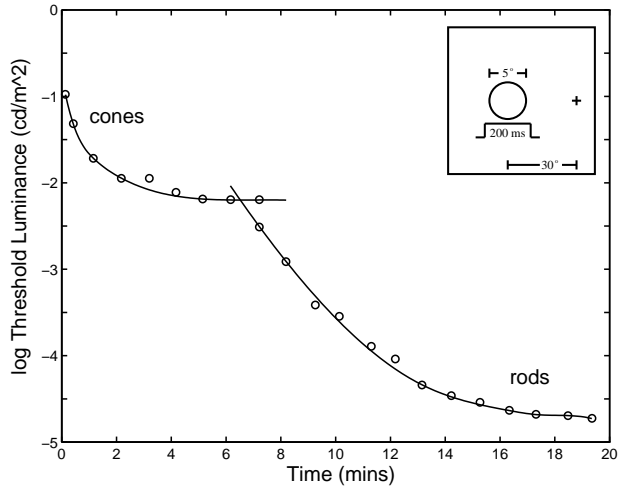


Figure 10: The time course of dark adaptation. After Riggs (1971).

Rushmeier and Ward have taken fundamentally different approaches to the tone reproduction process. Tumblin and Rushmeier’s brightness-based operator seeks to match suprathreshold brightness appearance across the range of scene luminances. On the other hand, Ward’s contrast-based operator, seeks to match contrast visibility at threshold and scales suprathreshold values relative to the threshold measure. Each approach has its strengths and weaknesses. A brightness-based operator may better capture the subjective appearance of surfaces in a scene, but it may not correctly capture the visibility of surfaces near threshold. Conversely, a contrast-based operator will correctly predict threshold visibility, but may not account well for suprathreshold appearance. A more complete model of tone reproduction for computer graphics may have to combine these two approaches to correctly account for *visibility at threshold* as well as *suprathreshold appearance*.

Because we have based our adaptation model on threshold data, our implementation is based on Ward’s concept of matching just noticeable differences for the world and display observers. Ward’s tone reproduction operator is:

$$L_d(L_w) = mL_w, \quad (1)$$

where L_w is the luminance seen by the world observer, and L_d is the luminance that L_w is mapped to on the display device. The multiplier m is chosen to achieve matches in visibility for the world and display observers. To achieve this, Ward assumes that we have a t.v.i. function $t(L)$ that gives a threshold luminance that is barely visible for a given adaptation luminance L . He further assumes that we have a way to estimate the adaptation luminance L_{wa} for the world observer and L_{da} for the display observer. This means that his multiplier m is a function of the adaptation levels of world and display observer. So he chooses $m(L_{wa}, L_{da})$ such that:

$$t(L_{da}) = m(L_{wa}, L_{da})t(L_{wa}), \quad (2)$$

so

$$m(L_{wa}, L_{da}) = t(L_{da})/t(L_{wa}). \quad (3)$$

This determines how luminance is mapped. Ward assumes that the chromatic channels follow the same mapping.

To construct our operator we first apply Ward’s model without change using our cone t.v.i. data from Figure 3, which is approximated by:

$$\log t_p(L_a) = \begin{cases} -0.72 & \text{if } \log L_a \leq -2.6, \\ \log L_a - 1.255 & \text{if } \log L_a \geq 1.9, \\ (0.249 \log L_a + 0.65)^{2.7} - 0.72 & \text{otherwise.} \end{cases} \quad (4)$$

This operator would work much the same as Ward’s model, although Equation 4 is slightly different from Ward’s because it is derived from different experimental data. We chose this data because we did not have access to the raw data Ward used, and because the differences are small enough that they are probably not significant.

We now extend Ward’s model to include the rod t.v.i. function shown in Figure 3. Our approximation to this data is:

$$\log t_s(L_a) = \begin{cases} -2.86 & \text{if } \log L_a \leq -3.94, \\ \log L_a - 0.395 & \text{if } \log L_a \geq -1.44, \\ (0.405 \log L_a + 1.6)^{2.18} - 2.86 & \text{otherwise.} \end{cases} \quad (5)$$

Since we expect an achromatic response from the rod system, we produce only a grayscale mapping. We do this by applying Equation 3 using the t.v.i. curves from Equation 5 for the world observer and Equation 4 for the display observer, because the display observer is in a photopic state of adaptation. This would be a plausible tone reproduction operator to preserve visibility for a coneless observer (a “rod monochromat”). This technique was inspired by Meyer’s (1986) model for simulating the visual experience of color-defective viewers.

For photopic conditions we can apply the photopic tone reproduction operator. For scotopic conditions we can apply the scotopic operator. But what do we do for mesopic conditions? Simply adding the results of the photopic and scotopic operators would be a mistake, because for high mesopic levels the rods would produce quite a bright image, when in fact they are shutting down due to saturation. Instead, we generate both a photopic display luminance L_{dp} and a scotopic luminance L_{ds} , and combine them with the formula:

$$L_d = L_{dp} + k(L_a)L_{ds}, \quad (6)$$

where k is a constant that varies from 1 to 0 as the scotopic world adaptation level goes from the bottom to the top of the mesopic range. The rods rather than the cones have a multiplier because the rod system is losing sensitivity as the intensity increases toward the photopic range, while the cones are quiescent and in a ready state. Because the cones are ready to respond, we apply Equation 6 for all scene adaptation levels. This way, a red stoplight in a night scene will be displayed properly.

4.1 Acuity

Just as we want threshold contrast to be mapped between the world and display observers, we would like resolvable detail to be preserved as well. From the data shown in Figure 7, we can determine what spatial frequencies are visible to the world observer. We simply remove all spatial frequencies above this in the image we present to the display observer. Because we don’t want ringing in the displayed image, we use a Gaussian convolution filter whose power spectrum amplitude at the cutoff frequency is matched to the observer’s

threshold. Thus we remove frequencies in the image which would not be discernable to the world observer:

$$f^*(\omega_c(L_{wa})) = \frac{t(L_{wa})}{L_{wa}}, \quad (7)$$

where f^* is the Fourier transform of the convolution filter, and $\omega_c(L_{wa})$ is the threshold frequency for the world adaptation of the viewer. This way a high contrast scene grating at frequency $\omega_c(L_{wa})$ will be displayed at the threshold of visibility for the display viewer.

4.2 Light Adaptation

The detection threshold for an observer who suddenly enters a bright environment, is high relative to the threshold for an observer adapted to the bright environment. The t.v.i. data for this situation is shown in Figures 8 and 9. We can apply Equation 3 to make sure that only high contrasts are visible. Although this would be valid in terms of visibility, it would produce a dim appearance, which is the opposite of qualitative experience. This is because whenever Equation 3 raises the contrast threshold for the world observer, it does this by making m small, thus assuring a dim appearance on the display. To combat this we note that any linear model can be put in place of Equation 3, and visibility can still be preserved, but we gain a free parameter that can increase the qualitative accuracy of appearance. We keep the m multiplier and add an offset, so that contrast can be reduced and screen brightness can be adjusted separately:

$$L_d(L_w) = mL_w + b. \quad (8)$$

The multiplier m will still be set by the same formulas as above. However, b will be a function of time. Because we have no quantitative data to set b , we do the simplest thing possible: we set b such that

$$L_d(L_{wa}) = \text{constant over time.} \quad (9)$$

This means the overall luminance of the display will not change during the light adaptation process. We could adjust the value of b in an ad-hoc manner to create a “flash” immediately after the viewer changes viewing conditions. We choose not to do this because we want to preserve a “hands-off” objective model.

4.3 Dark Adaptation

The detection threshold for an observer who suddenly enters a dim environment is high relative to the threshold of an observer adapted to the dim environment. The procedure we used for light adaptation can be applied without change.

4.4 Determining adaptation luminances

When applying display equations such as Equation 3, the result depends on the choices of the adaptation states L_{wa} and L_{da} . In the absence of any obviously correct answer, we opt for the simplest choice. For the world adaptation we choose half the highest visible luminance. For the display observer we use half the maximum screen luminance (typically $80/2 = 40cd/m^2$). We have observed that the appearance of many displayed images can be improved by tuning the adaptation luminances, but we purposely avoid doing this because we want to maintain an automatic process based on psychophysical data.

5 Results

The panels of Figure 11 show the results of applying our model of visual adaptation to a simulated scene. The scene is an office that contains a Snellen chart, and a Macbeth Colorchecker chart used as a standard in color reproduction. The rendered image file was created using Monte Carlo path tracing with a spectral color model, diffuse illumination that is uniform across the visible spectrum, and the standard reflectivities for the Macbeth chart (Wyszecki 1982). Panel (a) shows the image produced by our model for a scene illuminated at $1000 cd/m^2$. This image simulates what the scene looks like under photopic conditions that approximate normal daylight levels. Notice that all the colors in Macbeth chart are bright and saturated, and that all the letters in the Snellen chart can be recognized. Panel (b) shows the scene illuminated at $10 cd/m^2$. This approximates dim interior lighting and is near the top of the mesopic range. Notice that the scene is darker overall, that some contrast has been lost, and that the colors are less saturated, but acuity is still good since all the lines on the Snellen chart are recognizable. Panel (c) shows the scene illuminated at $0.04 cd/m^2$. This is a moonlight level near the the mesopic/scotopic transition. Notice that the saturation of all the colors in the Macbeth chart is greatly reduced, and that the blues and greens have become completely achromatic. Notice also that visual acuity has dropped significantly, and that the smaller letters on the Snellen chart can no longer be identified. Panel (d) shows the scene illuminated at starlight levels of $0.001 cd/m^2$ near the lower threshold of vision. At this level detection is the primary function of vision. The ability to distinguish colors and details has been lost. Only the largest and highest contrast forms can be discerned. The differences in contrast, color appearance, and spatial resolution that can be observed across this set of images are a consequence of the adaptation-related changes in visual function that are captured by our model.

One particular visual phenomenon predicted by our model is the *Purkinje shift* in the relative lightness of reds and blues in the mesopic range (Minnaert 1954). The shift is due to the re-ordering of the relative sensitivities of the rod and cone systems at mesopic levels. The effect can be seen in the reversal of the lightnesses of the red and blue squares in the Macbeth chart. In panel (b) the scene is illuminated at $10 cd/m^2$ near the top end of the mesopic range. At this level the red square appears lighter than the blue square. In panel (c), illuminated at $0.04 cd/m^2$ near the bottom of the mesopic range the blue square now appears lighter than the red.

Figure 12 (a) shows an image sequence that simulates the changes in visual function over the time course of light adaptation. In the first frame of the sequence the scene is illuminated to a level of $0.1 cd/m^2$. In the second frame the light level has just been raised to $5623 cd/m^2$. Notice that much of the scene is washed out. Apparent contrast is reduced and the colors in the Macbeth chart appear desaturated. The subsequent frames show how the scene appears at intervals following the change in illumination level. Notice that apparent contrast and color gamut increase over time. The final frame shows the scene after 75 seconds of light adaptation. After this time, adaptation is almost complete and visibility, color appearance, and acuity are near their steady state photopic levels.

Figure 12 (b) shows an image sequence that simulates the changes in visual function over the time course of dark adaptation. In the first frame of the sequence the scene is il-

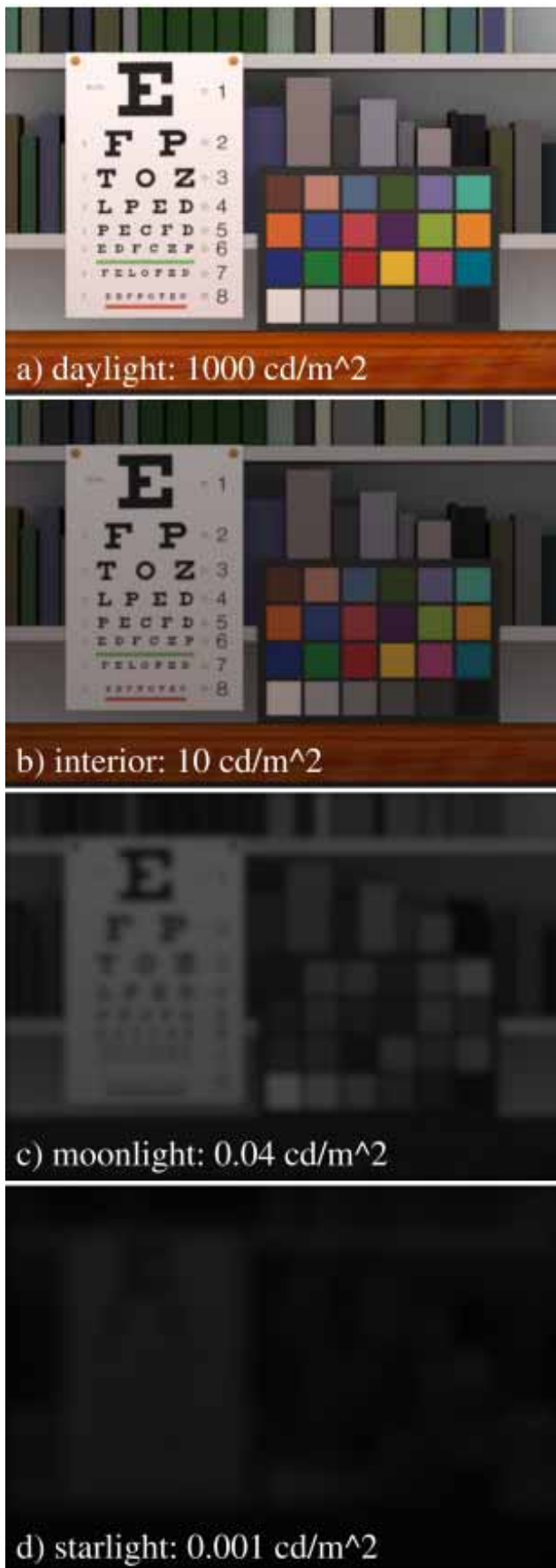


Figure 11: Visual function across the range of light.



Figure 12: (a) Image sequence showing the time-course of light adaptation; (b) Image sequence showing the time-course of dark adaptation.

illuminated to a level of 1412 cd/m^2 . In the second frame the light level has just been reduced to 0.1 cd/m^2 . Notice that at first the appearance is low contrast and that only the major scene features can be distinguished. The subsequent frames show how the scene appears at intervals during dark adaptation. The final frame shows the appearance after more than 3 minutes of dark adaptation. At this time adaptation is almost complete, and visibility, color appearance and acuity are close to their steady state scotopic levels.

6 Conclusions/Future Work

In this paper we have developed a computational model of the changes in visual function that are produced by adaptation. By applying this model to global illumination solutions we have generated images that better capture the visual appearance of scenes illuminated over a wide range of intensity

levels. Because this model is based on psychophysical experiments, the images produced are visually faithful representations and can be used predictively. However we must caution that since our data is derived from experiments conducted under widely varying conditions, none of which are likely to match typical viewing conditions, our images should be taken as approximations to a precisely accurate simulation.

There is still much work to be done in this area. While we have modeled the visual consequences of adaptation we still do not have a good model for a viewer's state of adaptation. This is a complex problem because the retina adapts locally and because eye movements cause the state of adaptation to change continuously.

We are also less than completely satisfied with our simulations of light and dark adaptation. While we believe our model predicts the changes in threshold visibility that occur over the time course of adaptation, we feel that our images do not completely capture the appearance of the early phases of light and dark adaptation. Our algorithm is based on Ward's contrast-threshold tone reproduction operator. Tumblin and Rushmeier have presented an alternative tone reproduction operator based on suprathreshold brightness measurements. Perhaps a more complete solution to the questions of adaptation-related changes in visibility and appearance will come from some combination of these models.

A more complete model of adaptation will be important for advances in realistic image synthesis. The quest for realism in computer graphics is pushing advanced software and hardware technology toward a convergence. On the software side are physically-based global illumination rendering methods that produce accurate simulations of the distribution of light energy in scenes. On the hardware side are high-resolution immersive displays in which computer generated images fill the visual field. True visual realism in image synthesis will eventually occur with the merging of these advanced technologies, but two problems stand in the way. First, current rendering methods are too slow to accommodate the real-time update rates required for immersive environments. Second, we do not know how to correctly display the results of global illumination simulations to produce realistic visual appearance in immersive display systems.

A better model of visual adaptation can help solve both of these problems. In the first case, an adaptation model can be used as the basis of perceptual error metrics to limit the precision of global illumination calculations based on visibility and appearance criteria. This could lead to time-critical global illumination rendering algorithms that achieve real-time rates. In the second case an adaptation model can be used to determine how to properly display images in immersive display systems where the display output fills the visual field and provides all the viewer's visual stimulation. Bringing these two techniques together in algorithms where rendering computations can be tightly constrained because the viewer's visual state is precisely known could lead to even greater computational efficiencies and greater visual realism.

Acknowledgements

Dan Kartch and Steve Marschner helped with the preparation of the paper and color figures. This work was supported by the NSF/ARPA Science and Technology Center for Computer Graphics and Scientific Visualization (ASC-8920219) and by NSF CCR-9401961 and performed on workstations generously provided by the Hewlett-Packard Corporation.

Bibliography

- Adelson E.H. (1982). Saturation and adaptation in the rod system. *Vision Research*, 22, 1299-1312.
- Aguilar, M. & Stiles, W.S. (1954). Saturation of the rod mechanism of the retina at high levels of stimulation. *Optica Acta*, 1, 59-65.
- Baker, H.D. (1949). The course of foveal adaptation measured by the threshold intensity increment. *Journal of the Optical Society of America*, 39, 172-179.
- CIE (1981). An analytic model for describing the influence of lighting parameters upon visual performance, vol. 1. Technical foundations. CIE 19/2.1, Technical committee 3.1.
- Crawford, B.H. (1947). Visual adaptation in relation to brief conditioning stimuli. *Proceedings of the Royal Society of London, Series B*, 128, 283-302.
- Granit R., Munsterhjelm, A., and Zewi, M. (1939). The relation between concentration of visual purple and retinal sensitivity to light during dark adaptation. *Journal of Physiology*, 96, 31-44.
- Hecht, S. (1934). Vision II: the nature of the photoreceptor process. In C. Murchison (Ed.), *A handbook of general experimental psychology*. Worcester, Massachusetts: Clark University Press.
- Hood, D.C. & Finkelstein M.A. (1986). Visual sensitivity. In K. Boff, L. Kaufman, & J. Thomas (Eds.), *Handbook of Perception and Human Performance (Volume 1)*. 5-1-5-66.
- IES (1993). *Lighting handbook: reference and application volume*, (8th edition). Mark S. Rea (Ed.). New York: Illuminating Engineering Society of North America.
- Meyer, G.W. (1986) Color calculation for and perceptual assessment of computer graphic images. Ph.D. thesis, Cornell University.
- Mueller, C.G. (1951). Frequency of seeing functions for intensity discrimination at various levels of adapting intensity. *Journal of General Physiology*, 34, 463-474.
- Minnaert, M. (1954) *The nature of light and color in the open air*. New York: Dover.
- Pugh, E.N. (1988). Vision: physics and retinal physiology, In R.C. Atkinson (Ed.), *Steven's handbook of experimental psychology*, (2nd edition). New York: Wiley.
- Riggs, L.A. (1971) Vision. In J.W. Kling & L.A. Riggs (Eds.), *Woodworth and Schlosberg's Experimental Psychology*, (3rd edition). New York: Holt, Rinehart, and Winston.
- Shaler, S. (1937) The relation between visual acuity and illumination. *Journal of General Physiology*, 21, 165-188.
- Spencer, G., Shirley P., Zimmerman, K. & Greenberg, D. (1995). Physically-based glare effects for computer generated images, *Proceedings ACM SIGGRAPH '95*, 325-334.
- Spillman, L., & Werner, J.S. (Eds.) (1990). *Visual perception: the neurophysiological foundations*. San Diego: Academic Press.
- Stevens, S.S., & Stevens, J.C. (1960). Brightness function: parametric effects of adaptation and contrast, *Journal of the Optical Society of America*, 53, 1139.
- Tumblin, J., and Rushmeier, H. (1993). Tone Reproduction for Realistic Images, *IEEE Computer Graphics and Applications*, 13(6), 42-48.
- Ward, G. (1994). A contrast-based scalefactor for luminance display. In P.S. Heckbert (Ed.), *Graphics Gems IV*, Boston: Academic Press Professional.
- Wyszecki G. & Stiles W.S. (1982). *Color science: concepts and methods, quantitative data and formulae (2nd edition)*. New York: Wiley.